Structure and dynamics of Ag clusters on Pt(111)

Carlo Massobrio and Philippe Blandin
Institut de Physique Expérimentale, Ecole Polytechnique Fédérale de Lausanne, PHB Ecublens, CH-1015 Lausanne, Switzerland
(Received 29 December 1992)

By using the embedded atom method potentials in the form derived by Foiles, Baskes, and Daw [Phys. Rev. B **33**, 7983 (1986)], we studied by static computations and molecular-dynamics (MD) simulations structural and dynamical properties of Ag clusters adsorbed on the (111) surface of Pt. Static computations were performed for clusters with up to 37 atoms and diffusion coefficients were evaluated for the adatom, dimer, and trimer at different temperatures. As shown by analyzing the trend of the dissociation energies with cluster size, the most stable structures on the surface are those formed by threefold-coordinated atoms, with dissociation energy $E^d \approx 0.45$ eV, while the presence of twofold-coordinated atoms at a given cluster size yields dissociation energies close to $E^d \approx 0.30$ eV. In particular, the largest dissociation energy is found for the heptamer, $E^d = 0.47$ eV. Calculated migration barriers are as low as $E_1^m = 0.05$ eV for the adatom, $E_2^m = 0.1$ eV for the dimer, and $E_3^m = 0.14$ eV for the trimer, thereby promoting enhanced mobility of these small structures at low temperatures. An Arrhenius plot of the diffusion coefficients up to $T = 800$ K gives a dynamical diffusion barrier of the adatom which is moderately larger than the static one, i.e., E_1^m (MD) $= (0.060 \pm 0.005)$ eV. Our results are consistent with recent experimental scanning-tunneling-microscopy findings on the early stages of growth of Ag on Pt(111) indicating the rapid formation of large silver islands at temperatures as low as $T = 200$ K.

I. INTRODUCTION

Atomistic scale computations, based on realistic N-body interatomic potentials, offer a unique tool to characterize structural and dynamical properties of clusters adsorbed on surfaces. In the case of transition metals the usefulness of such an approach is proved by a recent series of embedded atom method (EAM) computations in which the stable configurations of Pt and Pd clusters on Pt(100) (Refs. 1 and 2) and the general trend of activation energies for adatoms on a large variety of fcc metal surfaces[3] are found to be consistent with experimental observations. Moreover EAM computations were able to establish that self-diffusion on (001) fcc surfaces can indeed take place via an exchange between the diffusing adatom and an atom of the substrate,[4] as shown in the case of Pt by field-ion-microscope (FIM) experiments,[5] thereby indicating that relevant features of the diffusion mechanism are accessible to microscopic modeling. As further evidence a combination of FIM and EAM molecular static calculations were able to unravel the occurrence of both exchange and hopping in the mechanism of surface diffusion for Pt_2 and Pt_3 on Pt(100).[6]

In the case of (111) surfaces both homogeneous and heterogeneous systems have been modeled.[7–15] While in the Au/Ni(111) (Ref. 14) case the aim was to elucidate the relevance of misfit in determining the geometrical arrangements of large (up to 39 Au atoms) adsorbates, static computations of Ni_N/Ni(111) (Ref. 12) focused on the value of dissociation energies and migration barriers as a function of cluster size with the intent of relating to an experimental work performed on Ir_N/Ir(111).[16] The low value of diffusion barriers on (111) metallic substrates, typically in the range 0.05–0.2 eV, makes them particularly attractive for molecular-dynamics (MD) investigations, since the full details of the diffusion mechanism and a direct evaluation of the diffusion coefficients are, in principle, directly accessible to the time scales of MD simulations. Nevertheless, with the exception of a qualitative study on the behavior of a Lennard-Jones (LJ) dimer,[17] investigations of the dynamics of small clusters on (111) metallic surfaces are limited to the adatom case, as reported for Ag/Ag(111),[7,10] Rh/Rh(111),[10] and Ni/Ni(111).[11]

In this paper we elucidate structural and dynamical properties of Ag clusters on Pt(111) by making use of EAM interatomic potentials in the form presented in Ref. 20. Static computations are performed on Ag_N/Pt(111) for $1 \le N \le 37$, and MD simulations for $N = 1, 2, 3$. Our preliminary results from this model[15] focused on the relationship between diffusion properties and behavior upon collision on the surface of the dimer, which was directed on the (111) plane with impact energies of 0.5 and 5 eV. We were able to show that the enhanced mobility of Ag on Pt(111) favors the recovery of a stable dimer on the substrate by allowing the recombination of the constituent atoms separated by the collision.

Our concern here is to provide a detailed description of the elementary processes relative to the heterogeneous deposition of small metallic clusters on (111) metallic substrates, a parallel investigation on the behavior of larger adsorbates being currently in progress. Interest in cluster properties on (111) metallic surfaces is further motivated by experimental findings on the early stages of growth of Pt on Pt(111) (Ref. 18) which have been interpreted as a distribution of clusters of a particular size, the heptamer, in a way reminiscent of the "magic" sizes used to describe the arrangement of three-dimensional, unsupported metallic clusters. In addition, heteroepitaxy in

Ag/Pt(111) is currently investigated by scanning tunneling microscopy (STM) (Ref. 19) where large Ag two-dimensional islands are seen to form already at room temperature, indicating enhanced mobility and instability of small clusters, while at higher temperatures Ag and Pt atoms are found to interdiffuse at the step edges.

This paper is organized as follows. In Sec. II we describe the implementation of the model and the computations performed, for both static and dynamical investigations. Section III A is devoted to the results for the most stable structures of clusters with up to 37 atoms which are searched by relaxing the whole substrate/adsorbate system and then characterized in terms of geometrical arrangements as well as cohesive and dissociation energies. We also evaluate static diffusion barriers for Ag clusters with up to three atoms. Section III B contains an analysis of the diffusion mechanism based on MD simulation carried out at several temperatures as well as direct estimates of the diffusion coefficients. Conclusion and final remarks are presented in Sec. IV.

II. MODEL AND COMPUTATIONS

Both Ag and Pt are modeled by using EAM interatomic potentials implemented for fcc transition metals by Foiles, Baskes, and Daw.[20] The spherically averaged free-atom densities are taken in the double-ζ form from Refs. 21 and 22, respectively, for Ag and Pt. In most of our simulations we employed cutoffs for both attractive and repulsive parts equal to $R_c = 6$ Å, although it should be stressed that the embedding functions of Ref. 20 are correctly reproduced only by shifting $F(\rho)$ (the embedding part of the potential) and the repulsive part so as to be continuous at a cutoff $R_c \approx 5.2$ Å which includes three shells of neighbors. Our results proved to be insensitive to these small changes. When tested against the properties of the isolated Ag dimer the EAM potential turned out to be too attractive, with an equilibrium distance shorter than the experimental one[23] ($r_d = 2.27$ Å against $r_d^{\text{expt}} = 2.47$ Å) and a binding energy larger ($E_b = 1.385$ eV/atom to be compared with $E_b^{\text{expt}} = 0.83$ eV/atom). Since we were also concerned with a realistic modeling of collision events for Ag dimers on the Pt(111) surface,[15] we added to the repulsive Ag-Ag potential an interaction E_r' of the kind $E_r' = A \exp -(r - r_d)\lambda$, where A and λ are adjustable parameters, ranging up to R_c to reproduce experimental cohesive energy and equilibrium distance of Ag_2. The optimal choice of A and λ ($A = 0.28$ eV, $\lambda = 12$ Å^{-1}) modifies slightly the equilibrium condition of the bulk, since a lattice parameter 1% larger is needed to recover the equilibrium condition. The calculated vibrational frequency of Ag_2 is equal to 6.21×10^{12} Hz, in fair agreement with the experimental value[23] of 5.76×10^{12} Hz.

Given the inadequacy of EAM to describe isolated metallic clusters of small sizes we do not expect the inclusion of E_r' to improve the description of bonding and energetics in Ag_3. The EAM binding energy of isolated Ag_3 turns out to be 1.54 eV/atom when A and λ take the above values, and equal to 1.65 eV when $A = 0$ at the equilibrium distance $r_d = 2.55$ Å. These energies are much too high when compared to both experimental[24] and density functional[25] results. For equilibrium studies of clusters adsorbed on surfaces these flaws of the potential are not serious limitations since the environment affecting the cluster, strongly influenced by the presence of the substrate, has little to do with that pertaining to an isolated cluster. Accordingly we used the above modified EAM potentials in computations for all cluster sizes.

In our static computations we employed a slab of 4032 Pt atoms arranged in a parallelepipedic box with X, Y, and Z directions along the [110], [$\bar{1}\bar{1}2$], and [111] crystallographic axes, respectively. Periodic boundary conditions are imposed only in the X and Y directions. To minimize the interaction between the Ag cluster lying on the Pt(111) surface and its periodic images we considered fairly extended (111) planes, containing 336 atoms each. Hence the simulation cell consists of a repetition of 12 planes stacked according to the ABC-fcc sequence with interplanar distance $d_p = a/\sqrt{3}$, a being the lattice parameter, and edge lengths $L_x = 14a/\sqrt{2}$, $L_y = 12a\sqrt{3}/2$, $L_z = 4a\sqrt{3}$. The stacking sequence along the (111) direction defines in a natural way the position of an atom lying on the top of the Pt slab. By defining the uppermost Pt plane as a B plane, i.e., a plane made of atoms occupying sites of the B kind in a triangular lattice arrangement, the Ag adatoms will occupy upon relaxation either C sites, corresponding to a bulk site continuing the fcc structure, or a surface A site as in the hcp structure. Figure 1

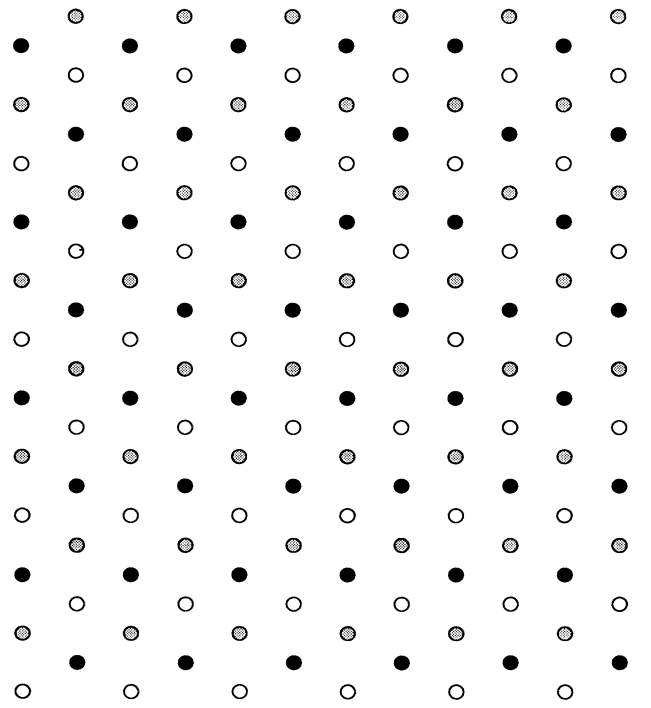

FIG. 1. Top view of a fcc (111) plane showing the location of three different types of sites corresponding to the ABC-fcc stacking along the [111] direction. With respect to the convention adopted in the text one can distinguish A sites (open circles), B sites (shaded circles), and C sites (filled circles).

displays the topology of the (111) plane and the position of the A, B, and C sites. Adsorption energies E_N^a are simply calculated by subtracting the total energy E_0^t of the Pt(111) slab from the total energy E_N^t of the Ag_N/Pt(111) system. The cluster cohesive energy on the surface E_N^c is commonly defined as N times smaller than the adsorption energy. In the following we make use also of the dissociation energy E_N^d given by $-(E_N^t - E_{N-1}^t - E_1^a)$.

To calculate adsorption energies the cluster atoms are initially placed at a distance d_p above the uppermost Pt(111) in C or A sites and then the whole system is allowed to relax under the action of a conjugate gradient energy minimization procedure. For example, the ground state of Ag_2/Pt(111) is searched by positioning first two Ag atoms at the largest distance compatible with periodic boundary conditions on the (111) plane and then in the C-C, A-A, and C-A configurations at initial distances $a/\sqrt{2}$, $a/\sqrt{2}$, $a/\sqrt{2/3}$. Static barriers relative to the bridge crossing between C (or A) and A (or C) sites are obtained similarly by constraining the moving atom at a given location in the XY plane along the diffusion path with the rest of the system relaxing at $T=0$ K. In the case of (111) surfaces the C-A hopping is known to be the elementary mechanism responsible for diffusion (at least at low temperatures) and the diffusion path for a cluster atom can be taken as the straight line joining two neighboring C and A sites. For polyatomic substrates the static computation of the migration energy, described in detail by Liu and Adams,[12] is based on the search of the lowest-energy barrier for migration of the clusters. To this end, all jumps compatible with long-range diffusion have to be determined, as well as the subsequent jumps required for cluster reforming. The migration energy for a given displacement is then the difference between the saddle-point energy and the energy relative to the equilibrium position of the adatom.

The system used for MD computations was smaller, containing 576 Pt atoms arranged in the geometry described above with 48 atoms in each one of the (111) planes. Equations of motion are solved via the velocity version of the Verlet algorithm[26] in the microcanonical ensemble with time step $\Delta t = 1.4 \times 10^{-15}$ s. This allows one to describe the diffusion mechanism and evaluate both the diffusion coefficients and the migration barriers, or "dynamical" diffusion barriers, for the Ag adatom, dimer, and trimer on Pt(111).

III. RESULTS

A. Static computations

Cohesive energies have been obtained at $T=0$ K for a series of substrate/adsorbate systems containing up to 37 Ag atoms. Some of the most stable structures of Ag_N on Pt(111) are given in Fig. 2, in particular for $1 \le N \le 7$, $N=10$, 13, and 19. The atomic positions refer to the beginning of the relaxation. In the C site the adatom is more stable than in the A site by 0.001 eV. The lowest energy for Ag_2/Pt(111) corresponds to atoms in C-C or A-A positions (C-C being favored by 0.003 eV) with equilibrium distance $r_d = 2.84$ Å, while the C-A configuration is higher by 0.04 eV, with $r_d = 2.88$ Å. The adsorption energy is $E_1^a = -2.7$ eV for the adatom and $E_2^a = -5.58$ eV for the dimer. Compact islands turned out to be lower in energy than linear chains, with an energy difference of 0.17 eV for the trimer rising to 0.5 eV for Ag_6.

The trends of cohesive and dissociation energies are given in Figs. 3 and 4, respectively. Two sets of geometrical arrangements have been considered for $N > 10$. In the first, larger clusters up to 19 (shown in Fig. 2) and then up to 37 are formed by completing two concentric shells of atoms around the heptamer so as to achieve compact hexagons, while in the second an elongated 13-

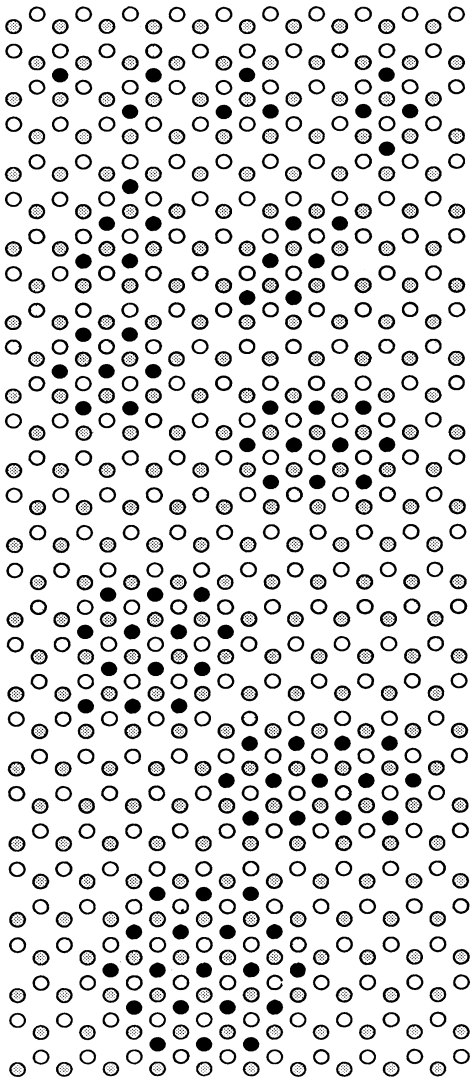

FIG. 2. Stable structures of Ag clusters on Pt(111) for $N=1,2,3,4,5,6,7,10,13$ (two geometrical arrangements are shown), $N=19$. For $N=13$ we display, from top to bottom, a structure obtained by completing a compact hexagonal shell around the heptamer and an elongated structure obtained from Ag_{10} by adding three atoms in the nearest-neighbor positions along the [110] direction.

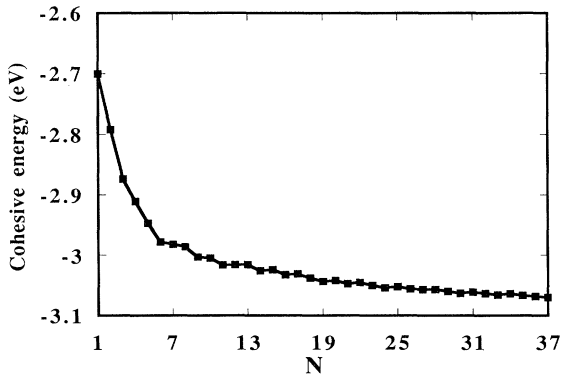

FIG. 3. Cohesive energy for Ag clusters on Pt(111). N is the number of atoms forming the cluster. The cohesive energy is the difference between the total energy of the system adsorbate plus substrate and the total energy of the substrate alone, divided by N.

atom structure is obtained by adding to Ag_{10} three atoms in the nearest-neighbor positions along the [110] direction. Among the two structures we considered for $N=13$, both shown in Fig. 2, the latter turned out to be lower in energy by 0.01 eV. While the cohesive energy decreases rapidly to an asymptotic value lower than the bulk cohesive energy [$E^c_{\rm bulk}(\mathrm{Ag})=-2.85$ eV], the dissociation energy (Fig. 4, upper side) is characterized by pronounced peaks which are the signature of the alternation between structures in which every atom has three nearest neighbors, i.e., it is threefold coordinated, and structures with one or two atoms are twofold coordinated. In particular it appears easier to remove an atom from Ag_{13} when the cluster is in the concentric shell configuration while Ag_{12} is less stable against dissociation in the elongated structure. A first pronounced peak at $N=7$ is consistent with simple geometrical arguments, as confirmed by data of dissociation energy per bond given in Ref. 18 and by two sets of independent computations performed on Ni/Ni(111),[12,27] whereas experimental data on Ir/Ir(111) (Ref. 16) display a more steady increase going from $N=4$ up to $N=7$. The stability of highly symmetric structures in which all atoms are threefold coordinated and the strength of the nearest-neighbor interaction in clusters with twofold-coordinated atoms have been recently invoked to interpret experimental findings[18] on the initial stages of growth of Pt on Pt(111). In Ref. 18 it was indeed suggested that the stability of the heptamer at a given temperature and coverage may be due to its compact geometrical arrangement and to the fact that the effective dissociation energy per bond decreases with increasing cluster size. This latter feature is partially confirmed by the data shown in the bottom part of Fig. 4, where the ratio of E^d_N to the number of bonds to be broken to remove an atom turns out to be lower for Ag_8 than for Ag_3 and Ag_5, but higher for Ag_9 than for Ag_5.

With increasing size the nearest-neighbor distance in Ag clusters approaches the bulk value ($r_d=2.886$ for Ag_{37}) and the cluster assumes a tentlike shape, with the atoms at the center of the cluster higher than the edge atoms, as shown in the upper part of Fig. 5, where the positions of the cluster atoms normal to the plane are given as a function of the distance from the central atom in Ag_{19} and Ag_{37}. As represented in the bottom part of Fig. 5, larger variations between the lowest and the highest atom in the cluster are found when one (or two) atoms in the cluster are twofold coordinated, the latter being systematically pulled closer to the surface. Furthermore the Pt atoms of the uppermost Pt(111) plane, which are nearest neighbors of the central Ag atom, move up by as much as 0.1 Å in the case of Ag_{37}. These trends are similar to what was found in a previous investigation of the Au/Ni(111) (Ref. 14) system, where the important misfit between the adsorbate and substrate lattice parameters causes the Au atoms at the edge of the

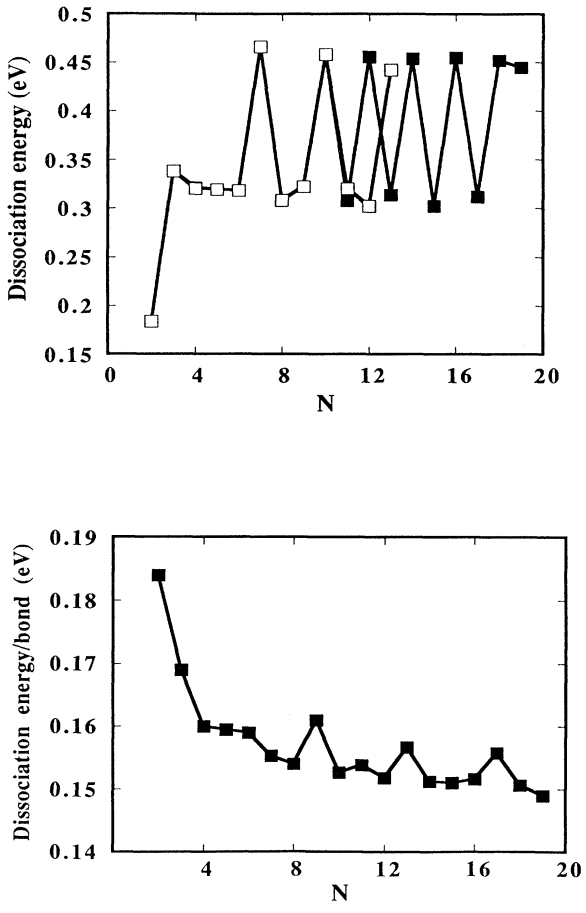

FIG. 4. Top: Dissociation energy of Ag clusters on Pt(111). For N up to 13 we show two sets of data, identical up to $N=10$, referring to the different geometrical arrangements used to build the clusters for $N=11,12,13$. Open squares: elongated structure, with Ag_{11} and Ag_{12} having twofold-coordinated atoms. Filled squares: concentric shell structure, with one twofold-coordinated atom found in Ag_{11} and Ag_{13}. Bottom: Effective dissociation energy per bond, obtained by dividing the dissociation energy by the number of bonds necessary to remove the least coordinated atom. Only the data referring to the concentric shell arrangement are reported.

cluster to be pushed away from the center towards stacking fault positions. This behavior is absent in our system where the edge atoms move radially outward by no more than 0.2 Å for the largest size of Ag cluster ($N=37$) we considered, the saddle point being $a/\sqrt{24}\approx 0.8$ Å far apart from the initial positions.

The diffusion barrier for the migration of Ag adatoms via the bridge hopping between the C and A sites is $E_1^m=0.05$ eV. Diffusion barriers for transition-metal adatoms on (111) transition-metal surfaces, typically ranging between 0.05 and 0.15 eV, have been recently obtained in the framework of N-body interatomic potential computations,[7–13] while available experimental data indicate larger values in the case of Ni/Ni(111),[28] Rh/Rh(111),[29] Ir/Ir(111).[16] It is worth mentioning, however, that the effective medium scheme gives values for the diffusion barriers of Cu on Cu(111) (Ref. 9) and Ag on Ag(111) (Ref. 8) which are about twice as large as the EAM values[3] and for Ag substantial agreement is found with the experimental results (0.12 eV against 0.15 ± 0.10).[8] In the case of Pt/Pt(111) a value of $E_1^m=0.23$ eV,[18] claimed to be consistent with effective medium computations,[13] was recently estimated on the basis of the observed mobility of Pt atoms at a 1-min scale at 80 K, while the EAM result obtained by using the interatomic EAM potential by Voter and coworkers[3,30] is three times smaller and the original scheme of Ref. 20 gives a completely unrealistic result[3] ($E_1^m=0.007$ eV). In our case recent STM results[19] yield for Ag/Pt(111) a diffusion barrier equal to $E_1^m=(0.096\pm0.012)$ eV, thereby indicating satisfactory accordance between experiments and calculations and confirming the tendency of the original EAM scheme to underestimate diffusion barriers on (111) transition-metal surfaces.

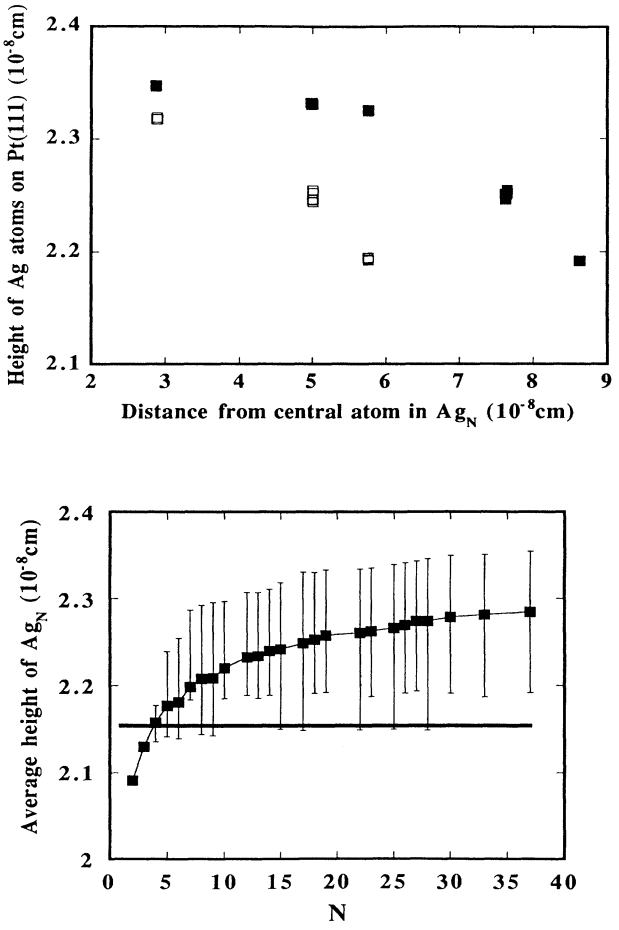

FIG. 5. Top: Heights of the Ag atoms in the clusters as a function of the distance from the central atom in Ag_{19} (open squares) and Ag_{37} (filled squares) on the uppermost Pt(111) plane, calculated with respect to the average height of the Pt plane. Bottom: average heights of Ag clusters on Pt(111). The bars indicate the range of variation in the atomic positions. The horizontal line is drawn at a height corresponding to the interplanar distance separating the two uppermost Pt layers in the relaxed configuration at $T=0$ K.

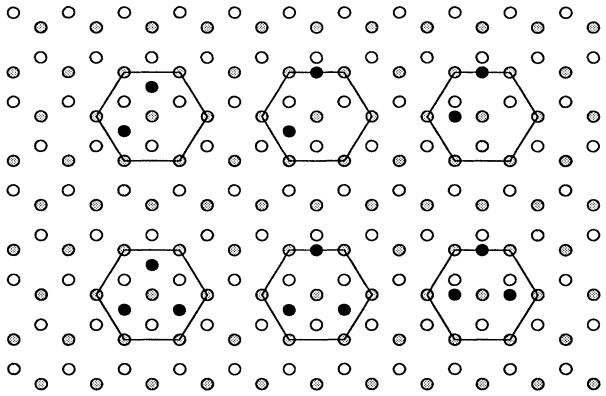

FIG. 6. Atomic configurations relative to the static computation of migration barriers. From left to right: (a) stable configuration of dimer (upper part) and trimer (lower part) on the (111) plane, (b) saddle point for the computation of the migration barrier relative to long-range intercellular diffusion, and (c) final configuration upon relaxation. Dimer and trimer atoms are represented by filled circles. Long-range diffusion requires the movement of the atoms promoting diffusion out of the hexagon highlighted in the figure.

We calculate the migration barrier of the dimer by moving one atom to the saddle point according to the configurations depicted in Fig. 6. This mechanism leads to intercellular movement which is necessary to promote long-range diffusion and corresponds to a barrier $E_2^m=0.10$ eV. The relaxation process, characterized by an accompanying movement of the companion atom along the direction of the diffusion path, ends with two Ag atoms at the equilibrium interatomic distance $\tau_d=2.84$ Å. A similar behavior was found in the case of the trimer, where this time two atoms move up in the direction of the diffusion path (see Fig. 6). The diffusion barrier for trimer long-range diffusion was found to be as low as $E_3^m=0.14$ eV.

B. Diffusion mechanism and dynamical barriers

We performed extended MD computations lasting up to 10^{-8} s with the intent of describing the diffusion mech-

anism for the silver adatom, dimer, and trimer on Pt(111) and evaluated their diffusion coefficients. It is useful to analyze the nature of the adatom movement by incrementing at a given atomic position, either a residence time, which is the time spent in the vicinity of a given adsorption site, or a flight time corresponding to the time spent in transit between two adsorption sites. In our case the adsorption sites are the A and C sites visited by the adatom moving at a given temperature on the uppermost Pt(111), and the residence time increases whenever the adatom is found within a distance $R_d = 0.4$ Å of an adsorption site.

One of the first results provided by our simulations is the existence of an elementary mechanism of diffusion consisting of a series of displacements between A and C adsorption sites. These jumps are highly correlated, as evidenced by the high percentage (20%) of back and forth jumps common to all temperatures, ranging from $T = 140$ to 800 K in the case of the adatom. Moreover the flight time is far from negligible, increasing from 10% at $T = 140$ K to 40% of the temporal trajectory at $T = 300$ K, thereby making the notion of jump frequency inaccurate to determine the diffusion barrier. For these reasons we calculate directly the diffusion coefficients D from the asymptotic behavior of the mean-square displacement in the form

$$D = \lim_{t\to\infty} D(t) = \lim_{t\to\infty} \frac{\langle R^2(t)\rangle}{4t} , \tag{1}$$

where $R^2(t)$ refers to the center of mass in the case of the dimer and trimer. We display in Figs. 7 and 8 the trends of $D(t)$ relative to the adatom at different temperatures along a time interval of 10 ps. The statistical errors reported are standard deviations of the mean obtained by partitioning the trajectory in subsections of 10^{-10} s each. At the lower temperatures, $T = 140$ and 185 K, diffusion on the compact (111) surface turns out to be a process characterized by a long relaxation time with $D(t)$ decreasing by as much as 30% and 15%, respectively, in between 2 and 4 ps. The establishment of a plateau requires

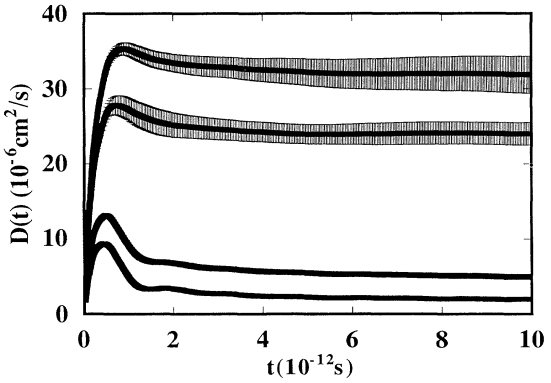

FIG. 7. Temporal behavior of the quantity $D(t) = \langle R^2(t)\rangle/4t$ with estimated error bars at four different temperatures for Ag/Pt(111). From bottom to top, $T = 140$, 185, 300, and 360 K.

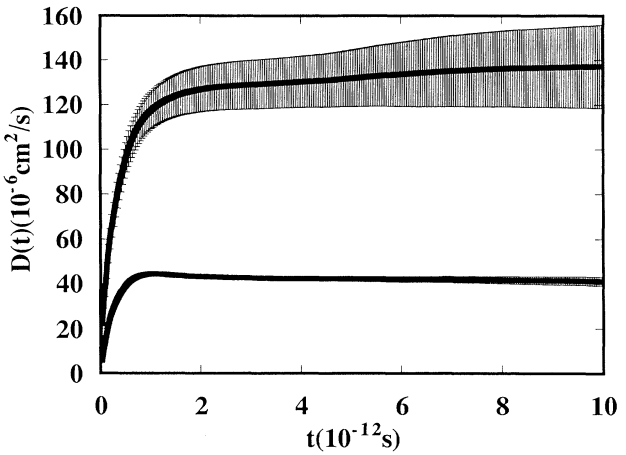

FIG. 8. Temporal behavior of the quantity $D(t) = \langle R^2(t)\rangle/4t$ with estimated error bars at temperatures $T = 420$ and 800 K for Ag/Pt(111). From bottom to top, $T = 420$ and 800 K.

a time of the order of $t^* = 6$ ps, as shown in Fig. 7 where for $t > t^*$ the values of $D(t)$ lie within the error bar estimated at $t = t^*$. $D(t)$ drops more smoothly at larger temperatures, decreasing by no more than 2% of the maximum value at $T = 360$ K. On the other hand, at $T = 800$ K (see Fig. 8) a steady increase is observed throughout the interval spanned by our statistical average and the attainment of a plateau value appears to be beyond the time scale of our computations. Nevertheless, the asymptotic behavior of $D(t)$, clearly appearing in Fig. 8, legitimates the choice of $D(t = 10$ ps) as a representative value for the diffusion coefficient at that temperature.

The diffusion coefficients plotted in an Arrhenius form are shown in Fig. 9, with dynamical migration barriers, i.e., the slopes of $\ln D$ vs $1/T$, given by $E_1^m(\mathrm{MD}) = (0.060 \pm 0.005)$ eV for the adatom, $E_2^m(\mathrm{MD}) = (0.09 \pm 0.01)$ eV for the dimer, and $E_3^m(\mathrm{MD}) = (0.13 \pm 0.01)$ eV for the trimer. These values are essentially identical to those calculated via static computations, with the exception of the adatom for which $E_1^m(\mathrm{MD}) > E_1^m$. In this context it is worth re-

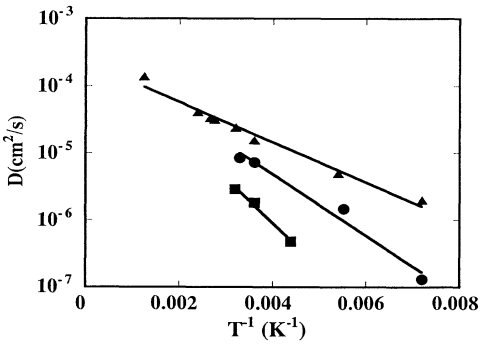

FIG. 9. Diffusion coefficients of silver adatom (triangles), dimer (circles), and trimer (squares) on Pt(111) displayed in an Arrhenius form as a function of temperature.

calling that large differences between dynamical and static barriers were found in recent MD diffusion studies of Ag on Ag(111) and Rh on Rh(111) [E_1^m(MD)=(0.055±0.011) eV against E_1^m=0.028 in the case of silver],[10] where diffusion coefficients were included in a single Arrhenius plot for temperatures in the range $200 \leq T \leq 600$ K. Although our results do not support such an effect, it is interesting to note that the dynamical barrier for the adatom in our case takes the value E_1^m(MD, low T)=(0.052±0.005) eV when only the data up to T=300 K are considered, while in the high-temperature region, for $300 < T \leq 800$ K the Arrhenius plot gives E_1^m(MD, high T)=(0.08±0.01) eV. This suggests that as the temperature increases a mechanism different from a jumplike behavior gradually sets in, in a way consistent with our simple observation that the residence time on the adsorption sites decreases with increasing temperature.

The diffusion mechanisms for the dimer and trimer have been further elucidated by following the evolution of the interatomic distances r_d. In agreement with the FIM observations of Wang and Ehrlich[16] the movement of the dimer at least at low temperatures can be expressed as the result of a combination of intracellular and intercellular individual jumps between C and A adsorption sites. The first diffusion mode corresponds to a rotational movement within the hexagonal cell made of B sites represented in Fig. 6 and consists in a sequence of C-C, C-A, and A-A configurations with r_d remaining between 2.7 and 3.0 Å. Intercellular movement, which is responsible for long-range diffusion, occurs when one atom crosses the saddle point to move out of the cell from a C (or A) site to an A (or C) site, while the other follows it, to occupy a stable site. Throughout this process the interatomic distances can be found in the range $3.2 < r_d < 3.6$ Å. In a similar way long-range diffusion of the trimer is promoted by individual atomic displacements out of the hexagonal cell with the triangular configuration preserved by a succession of C-A concerted displacements of the other Ag atoms. No interconversion between triangular and linear configurations is observed.

In Fig. 10 we display the distribution of interatomic distances r_d resulting from the movement of Ag_2 and Ag_3 on the surface. At T=140 K the dimer moves via a series of concerted individual hops between C and A adsorption sites, mostly reflecting intracellular movement. Long-range diffusion is very limited as indicated by the low value of the diffusion coefficient, $D \approx 10^{-7}$ cm^2/s, which corresponds to a distance of only 10 Å covered by the center of mass along the interval spanned in our simulation. As shown in Fig. 10, diffusion is enhanced at T=300 K where a significant fraction of time is spent by the dimer, as well as by the trimer, in intermediate C-A (or C-A-A for the trimer) configurations leading to intercellular displacements. Dissociation occurs after 10^{-9} s at T=320 K for the dimer and T=410 K for the trimer. These values, together with the assumption of a prefactor equal to h/KT (h being the Planck constant) allow us to recover dissociation energies equal to 0.22 eV for the dimer and 0.35 eV for the trimer, in fair agreement with

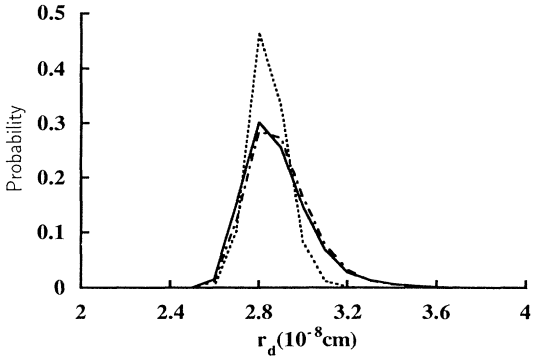

FIG. 10. Histogram of distribution of interatomic distances r_d in silver dimer and trimer moving on Pt(111) at different temperatures. Dotted line: Ag_2 on Pt(111) at T=140 K. Full line: Ag_2 on Pt(111) at T=300 K. Dashed-dotted line: Ag_3 on Pt(111) at T=300 K.

the values E_2^d=0.18 eV and E_3^d=0.34 eV obtained by static computations (see Fig. 4). Ag_2 and Ag_3 are therefore unstable on Pt(111) at temperatures $T > 300$ K and $T > 400$ K, respectively, at least on the time scale of our computations. On a time scale of 1 s, this would imply the dimer to be unstable at temperatures $T > 85$ K and the trimer at $T > 140$ K. Although our results refer to the behavior of a single cluster moving on an otherwise perfect periodic surface and cannot be compared directly to experimental results, it is useful to point out their consistency with recent STM measurements on the Ag/Pt(111) system indicating the dissociation of Ag_2 and Ag_3 at temperatures as low as T=150 K (Ref. 19) and the subsequent rapid formation of larger islands.

IV. CONCLUSIONS

The main objective of this work is to characterize the behavior of adsorbed Ag clusters on Pt(111) through the computation of structural and dynamical properties in the framework of the EAM description of interatomic interactions. Our computations, which are based on a slightly modified form of the original EAM scheme adapted to reproduce the properties of isolated Ag dimers, proved that two-dimensional arrangements where all atoms are threefold coordinated are the most stable structures, as shown by the trend of the dissociation energy which displays a first marked peak for N=7 with E_7^d=0.47 eV and then an alternation of values close to either $E^d \approx 0.45$ eV (structures with threefold-coordinated atoms only) or $E^d \approx 0.30$ eV (structures with one or two atoms twofold coordinated).

The diffusion barriers turn out to be as low as E_1^m=0.05 eV for the adatom, E_2^m=0.1 eV for the dimer, and E_3^m=0.14 eV for the trimer when obtained via static computations. Molecular-dynamics computations of the asymptotic temporal trends of mean-squared displacements and an Arrhenius representation of the resulting diffusion coefficients as a function of temperature indicate that in the case of the adatom the "dynamical" migration barrier is slightly larger, i.e., E_1^m(MD)=(0.060±0.005)

eV for the adatom. Long-range diffusion is promoted by individual intercellular displacements of one of the cluster atoms which crosses the saddle-point barrier hopping from one fcc-like site to a hcp-like site (and vice versa), thereby moving out of the hexagon formed by the neighboring Pt atoms lying on the uppermost (111) plane.

Two combined observations indicate the onset of a diffusion mechanism for the adatom at high temperatures which is intrinsically different from the jumplike behavior characteristic at low temperatures, as first pointed out in the context of an analysis of adatom and vacancy surface diffusion in a Lennard-Jones model.[31] First, the time spent by the adatom in transit between adsorption sites increases with increasing temperature, up to the point where the movement becomes a nearly free translation on the plane. Then the Arrhenius plot of diffusion coefficients relative to the region of low ($140 < T \leq 300$ K) temperatures gives a migration barrier significantly different from the one obtained by considering temperatures in the range $300 < T \leq 800$ K, i.e., E_1^m(MD, high T)$=0.08$ eV against E_1^m(MD, low T)$=0.052$ eV.

The main implication of the low diffusion barriers is an enhanced mobility of Ag small clusters on the surface, with diffusion coefficients which are as high as 2.4×10^{-5} cm^2/s for the adatom, 8.3×10^{-6} cm^2/s for the dimer, and 2.9×10^{-6} cm^2/s for the trimer at $T=300$ K. Since the dissociation energies we found are compatible with very short intervals of stability for such small clusters on the (111) plane even at low temperatures, the picture of the early stages of growth that emerges from our results points toward the existence of large islands which eventually, in an experimental situation, will nucleate at the step edges. Recent STM results[19] obtained for coverages of 0.1 monolayer are in agreement with this description and appear to indicate, at high temperatures, the further formation of heterogeneous structures on the uppermost (111) layer with dissolution of silver into the Pt surface layer proceeding from the lower side of the Pt step edges and restricted to the topmost layer. Work aimed at providing further numerical evidence in this direction is currently in progress.

ACKNOWLEDGMENTS

We wish to acknowledge useful discussions with Professor J. Buttet, Dr. P. Ballone, Dr. W. de Heer, Dr. H. Roeder, and Dr. K. Kern. In particular we wish to thank H. Roeder and K. Kern for providing us with their STM results on Ag/Pt(111) prior to publication.

[1]P. R. Schwoebel, S. M. Foiles, C. M. Bisson, and G. L. Kellogg, Phys. Rev. B **40**, 10 639 (1988).
[2]A. F. Wright, M. S. Daw, and C. Y. Fong, Phys. Rev. B **42**, 9409 (1990).
[3]C. L. Liu, J. M. Cohen, J. B. Adams, and A. F. Voter, Surf. Sci. **253**, 334 (1991).
[4]P. J. Feibelman, Phys. Rev. Lett. **65**, 729 (1990).
[5]G. L. Kellogg and P. J. Feibelman, Phys. Rev. Lett. **64**, 3143 (1990).
[6]G. L. Kellogg and A. F. Voter, Phys. Rev. Lett. **67**, 622 (1991).
[7]W. K. Rilling, C. M. Gilmore, T. D. Andreadis, and J. A. Sprague, Can. J. Phys. **68**, 1035 (1990).
[8]G. W. Jones, J. M. Marcano, J. K. Norskov, and J. A. Venables, Phys. Rev. Lett. **65**, 3317 (1990).
[9]L. Hansen, P. Stoltze, K. W. Jacobsen, and J. K. Norskov, Phys. Rev. B **44**, 6523 (1991).
[10]D. E. Sanders and A. E. DePristo, Surf. Sci. **264**, L169 (1992).
[11]C. L. Liu and J. B. Adams, Surf. Sci. **265**, 262 (1992).
[12]C. L. Liu and J. B. Adams, Surf. Sci. **268**, 73 (1992).
[13]J. K. Norskov, K. W. Jacobsen, P. Stoltze, and L. B. Hansen, Surf. Sci. **283**, 277 (1993).
[14]C. M. Gilmore, J. A. Sprague, J. M. Eridon, and V. Provenzano, Surf. Sci. **218**, 26 (1989).
[15]P. Blandin and C. Massobrio, Surf. Sci. **279**, L219 (1992).
[16]S. C. Wang and G. Ehrlich, Surf. Sci. **239**, 301 (1990).
[17]D. Ghaleb, Surf. Sci. **137**, L103 (1984).
[18]G. Rosenfeld, A. F. Becker, B. Poelsema, L. K. Verheij, and G. Comsa, Phys. Rev. Lett. **69**, 917 (1992).
[19]H. Roeder, H. Brune, J. P. Bucher, R. Schuster, and K. Kern (unpublished).
[20]S. M. Foiles, M. I. Baskes, and M. S. Daw, Phys. Rev. B **33**, 7983 (1986).
[21]E. Clementi and C. Roetti, At. Data Nucl. Data Tables **14**, 442 (1974).
[22]A. D. McLean and R. S. McLean, At. Data Nucl. Data Tables **26**, 305 (1981).
[23]K. P. Huber and G. Herzberg, *Molecular Spectra and Molecular Structure IV. Constants of Diatomic Molecules* (Van Nostrand, Princeton, 1979).
[24]K. Hilpert and K. A. Gingerich, Ber. Bunsenges. Phys. Chem. **84**, 739 (1980).
[25]W. Andreoni and J. L. Martins, Surf. Sci. **156**, 635 (1985).
[26]H. C. Andersen, J. Comput. Phys. **52**, 24 (1983).
[27]C. Massobrio (unpublished). We point out that in Ref. 12 Fig. 5(b) referring to the dissociation energy of Ni clusters is inconsistent with Fig. 5(a), which gives the binding energies. When the latter values are employed correctly to obtain dissociation energies, a behavior similar to the one displayed in Fig. 4 is recovered.
[28]R. T. Tung and W. R. Graham, Surf. Sci. **97**, 73 (1980).
[29]G. Ayrault and G. Ehrlich, J. Chem. Phys. **60**, 281 (1974).
[30]A. F. Voter and S. P. Chen, in *Characterization of Defects in Materials,* edited by R. W. Siegel, J. R. Weertman, and R. Sinclair, MRS Symposia Proceedings No. 82 (Materials Research Society, Pittsburgh, 1987), p. 175.
[31]G. De Lorenzi, G. Jacucci, and V. Pontikis, Surf. Sci. **116**, 391 (1982).